Materials Research Proceedings **26** (2023) 387-392 https://doi.org/10.21741/9781644902431-63

Direct dynamics of 2D cable-driven parallel robots including cables mass effect and its influence in the control performance

Guillermo Rubio Gómez[1,a *], Andrea Arena[2,b], Erika Ottaviano[3,c] and Vincenzo Gattulli[2,d]

[1]Industrial and Aerospace Engineering School, University of Castilla-La Mancha, Av. Carlos III s/n, 45004 Toledo, Spain

[2]Department of Structural and Geotechnical Engineering, Sapienza University of Rome, Via Eudossiana 18, Rome, 00184, Italy

[3]Department of Civil and Mechanical Engineering, University of Cassino and Southern Lazio, Via G. Di Biasio 43, Cassino, 03043, Italy

[a]guillermo.rubiogomez@uclm.es, [b]andrea.arena@uniroma1.it, [c]ottaviano@unicas.it, [d]vincenzo.gattulli@uniroma1.it

Keywords: Cable-Driven Parallel Robot, Nonlinear Modeling, Direct Dynamics, Distributed Mass Cable

Abstract. Cable-driven parallel robots are a type of parallel manipulators where rigid links are replaced by actuated cables. Although in many cases dynamic models that neglect the cables mass and elasticity are employed to simulate the robot behavior and test the control approach to be used, there are several situations in which their effect cannot be disregarded, especially when large span cables are used, and the cable mass density generates important cable sagging. This work proposes a dynamic model for planar cable-driven parallel robots with 3 degrees-of-freedom considering cables mass and elasticity. Furthermore, the effect of using control approaches based on massless inelastic cables dynamic models on robots with non-negligible cable mass and elasticity is finally assessed.

Introduction

Cable driven parallel robots (CDPR) are a special kind of parallel manipulators where rigid links are replaced by cables. By controlling the cables length, the position and orientation of the end-effector (EE) can also be controlled. These robots offer several advantages as the potential to cover large working areas and a very good power to weight ratio [1,2]. On the other hand, they also present disadvantages, one of them related to the complexity of the robot dynamic model. One common dynamic model used to analyze the dynamic behavior of CDPRs considers massless, inelastic cables, as in [3]. In this model, cables are considered as straight strings that transmit directly the cable tension generated by the winches to the end-effector, significantly reducing the complexity of the model. However, in some situations, these models do not represent the dynamic behavior of the robot with the required level of accuracy. These scenarios include large robots where, due to the cross-section and length of the cables, the cables mass cannot be neglected [4]. Static analyses were already performed by means of a geometrically exact model proposed in [5]. In this work, a dynamic model that considers cable mass and elasticity is proposed for planar CDPRs with 3 degrees-of-freedom (DOF) and n cables. The model proposed in this work is derived from a more comprehensive 3D model developed by the same authors of the present work in [6] where all the modeling details can be found. The model consists of a set of partial differential equations with boundary conditions modeling the cables behavior coupled with ordinary differential equations (ODE) that model the EE. A methodology for obtaining a solution to the

system is proposed, it is validated through numerical simulations and the influence of the cable mass is assessed in two case-study.

Nonlinear parametric modeling

Mechanical formulation

Let us consider $s_i \in [0, L_i(t)]$ $(i = 1, \dots, n)$ the arclength of the unstretched configuration, $L_i(t)$ is the total unstretched length and $l_i(t)$ the linear distance between the boundaries of the *i*-th cable. Vectors $\boldsymbol{x}_i = [y_i \; z_i]^\top$represent the positions of the cable origins in the robot structure w.r.t. the fixed reference frame $(\boldsymbol{e}_y, \boldsymbol{e}_z)$ located at $\boldsymbol{x}_1 \equiv \boldsymbol{0}$. The vector $\boldsymbol{r}_i(t) = \boldsymbol{R}_x(\theta_x(t)) \cdot \boldsymbol{r}_i^0$ represents the position of the *i*-th cable attachment point to the end-effector (EE) w.r.t the fixed reference frame $(\boldsymbol{e}_y, \boldsymbol{e}_z)$ while $\boldsymbol{r}_i^0$ is the vector describing the EE geometry in the mass-fixed local axes $(\boldsymbol{b}_y(t), \boldsymbol{b}_z(t))$ centered in the EE center of mass O_M, while $\theta_x(t)$ is the rotation angle about the axis $\boldsymbol{e}_x \equiv \boldsymbol{b}_x$ orthogonal to the working plane, and $\boldsymbol{R}_x$ is the rotation matrix around the x-axis. The position of O_M can be calculated as

$$\boldsymbol{p}_M(t) = \boldsymbol{p}_{M,i}(t) - \boldsymbol{r}_i(t) + \boldsymbol{x}_i (i = 1, \dots, n). \qquad (1)$$

The position of the point on the *i*-th cable is given by the vector $\boldsymbol{p}_i(s_i, t)$ w.r.t. $\boldsymbol{x}_i$. The strain state of the *i*-th cable can be described by introducing the stretch vector $\boldsymbol{\nu}_i(s_i, t)$ obtained as

$$\boldsymbol{\nu}_i(s_i, t) = \frac{d}{ds_i}\boldsymbol{p}_i(s_i, t). \qquad (2)$$

The vector of the cable axial force can be expressed as: $\boldsymbol{n}_i(s_i, t) = N_i(s_i, t)\boldsymbol{\nu}_i(s_i, t)/\nu_i(s_i, t)$, where $N_i(s_i, t) = EA(\nu_i(s_i, t) - 1)$ represents the cable tension, being EA the cable axial stiffness.

Nondimensional form

The distance $l_{0,1} = l_1(0)$ is adopted as characteristic length while the characteristic frequency $\omega_c = \sqrt{EA/(\rho A\, l_{0,1}^2)}$ is adopted to nondimensionalize the time. The following nondimensional parameters can be introduced

$$\lambda_{0,i} = \frac{l_{0,i}}{l_{0,1}}, \bar{x}_i = \frac{x_i}{l_{0,1}}, \bar{r}_i^0 = \frac{r_i^0}{l_{0,1}}, \bar{r}_i = \frac{r_i}{l_{0,1}}$$
$$\bar{\boldsymbol{p}}_M = \frac{\boldsymbol{p}_M}{l_{0,1}}, \; \bar{\boldsymbol{p}}_i = \frac{\boldsymbol{p}_i}{l_{0,1}}, \bar{\boldsymbol{n}}_i = \frac{\boldsymbol{n}_i}{\rho A \;\; \omega_c^2 \;\; l_{0,1}^2}, \; \tau = \omega_c \cdot t \qquad (3)$$
$$\lambda_i(\tau) = \frac{l_i(\tau)}{l_{0,i}}, \; \Lambda_i(\tau) = \frac{L_i(\tau)}{l_i(\tau)}, \; \sigma = \frac{s_i}{L_i(t)}, \; (i = 1 \dots n).$$

By defining $(\cdot)' := \frac{d}{d\sigma}(\cdot)$ and $(\dot{\cdot}) := \frac{d}{d\tau}(\cdot)$, as the derivatives in terms of the nondimensional arclength σ and time τ , respectively, the stretch vector can be then calculated as $\boldsymbol{\nu}_i(\sigma, \tau) = \bar{\boldsymbol{p}}_i'(\sigma, \tau)/(\Lambda_i(\tau)\lambda_i(\tau)\lambda_{0,i})$. Due to the definition of ω_c, it turns out that the *i*-th axial force is given in nondimensional form as $\bar{N}_i(\sigma, \tau) = (\nu_i(\sigma, \tau) - 1)$; therefore, the corresponding vector of the nondimensional axial force can be written as

$$\bar{\boldsymbol{n}}_i(\sigma, \tau) = \frac{1}{\Lambda_i(\tau)\lambda_i(\tau)\lambda_{0,i}} \frac{(\nu_i(\sigma, \tau) - 1)}{\nu_i(\sigma, \tau)} \bar{\boldsymbol{p}}_i'(\sigma, \tau). \qquad (4)$$

where $\nu_i = ||\nu_i||$. Finally, the equation of motion of the *i*-th cable in nondimensional form reads

$$\frac{\bar{\boldsymbol{n}}_i'(\sigma, \tau)}{\Lambda_i(\tau)\lambda_i(\tau)\lambda_{0,i}} + \bar{\boldsymbol{f}}_i(\sigma, \tau) = \ddot{\bar{\boldsymbol{p}}}_i(\sigma, \tau) + \bar{c}_i \dot{\bar{\boldsymbol{p}}}_i(\sigma, \tau) \; (i = 1, \dots, n), \qquad (5)$$

Materials Research Proceedings **26** (2023) 387-392 https://doi.org/10.21741/9781644902431-63

where $\bar{c}_i = c_i/(\rho A_1 \omega_c)$. The nondimensional distributed load, calculated as $\bar{\boldsymbol{f}}_i = \boldsymbol{f}_i/\left(\rho A_1 \omega_c^2 l_{0,1}\right)$, is here considered to be the only cable self-weight, therefore $\bar{\boldsymbol{f}}_i = -\gamma\, \boldsymbol{e}_z$, where $\gamma = g/\left(\omega_c^2\, l_{0,1}\right)$ and $g = 9.81\ m/s^2$ is the gravity acceleration. Furthermore, the kinematic boundary conditions associated with Eq. (5) can be written in nondimensional form as

$$\bar{\boldsymbol{p}}_i(0,\tau) = 0 \quad (i = 1, \dots, n), \qquad (6)$$

$$\bar{\boldsymbol{x}}_i + \bar{\boldsymbol{p}}_i(1,\tau) - \bar{\boldsymbol{r}}_i(\tau) = \bar{\boldsymbol{p}}_1(1,\tau) - \bar{\boldsymbol{r}}_1(\tau) \quad (i = 2, \dots, n), \qquad (7)$$

while the nondimensional form of the EE balance equations can be written as

$$-\sum_{i=1}^{n} \bar{\boldsymbol{n}}_i(1,\tau) - \mu\,\gamma\,\boldsymbol{e}_z = \mu\left(\ddot{\bar{\boldsymbol{p}}}_1(1,\tau) - \ddot{\bar{\boldsymbol{r}}}_1(\tau)\right), \qquad (8)$$

$$-\sum_{i=1}^{n} \left(\bar{\boldsymbol{r}}_i(\tau) \times \bar{\boldsymbol{n}}_i(1,\tau)\right) \cdot \boldsymbol{e}_x = \bar{J}_\mu\, \ddot{\theta}_x(\tau), \qquad (9)$$

respectively, where $\mu = M/\left(\rho A_1\, l_{0,1}\right)$ and $\bar{J}_\mu = J_M\left[1/\left(\rho A_1\, l_{0,1}^3\right)\right]$, being M and J_M the end-effector mass and mass moment of inertia, respectively.

Discretization procedure

The discretization technique based on the Galerkin method is adopted to reduce the space-dependence of the cables equations of motion so as to reduce them into a set of ordinary differential equations (ODEs), in τ. In this work $m+1$ trial functions are chosen so as to satisfy the kinematic boundary conditions (6) and (7); therefore, the approximate solution of Eq. (5) is given by the 2-by-1 vector $\tilde{\boldsymbol{p}}_i(\sigma,\tau)$ $(i = 1, \dots, n)$ expressed as the linear combination of the $m+1$ trial functions as

$$\tilde{\boldsymbol{p}}_i(\sigma,\tau) = \boldsymbol{q}_{i,0}(\tau)\,\sigma + \sum_{j=1}^{m} \phi_{i,j}(\sigma)\ \boldsymbol{q}_{i,j}(\tau), \qquad (10)$$

where $\phi_{i,j}(\sigma) = \mathrm{diag}\left(sin(j\pi\sigma), sin(j\pi\sigma)\right)$ is the ij-th 2-by-2 diagonal matrix collecting the j-th trial functions and $q_{i,0}$ and $q_{i,j}$ are the vectors collecting the unknown generalized coordinates. Since $\tilde{p}_i(0,\tau) = 0$, Eq. (10) satisfies (6), whereas, to satisfy Eq. (7), the following relationship must hold:

$$\boldsymbol{q}_{i,0}(\tau) = \boldsymbol{q}_{1,0}(\tau) - \bar{\boldsymbol{r}}_1 + \bar{\boldsymbol{r}}_i - \bar{\boldsymbol{x}}_i, \ (i = 2, \dots, n), \qquad (11)$$

since $\tilde{\boldsymbol{p}}_i(1,\tau) = \boldsymbol{q}_{i,0}$. Therefore, only one out of n vectors $\boldsymbol{q}_{i,0}(\tau)$ is an effective set of unknown coordinates. By now substituting (10) into (5) one obtains the following unbalanced residual of the equations of motion

$$\tilde{\boldsymbol{\eta}}_i(\sigma,\tau) = \frac{1}{\Lambda_i^2 \lambda_i^2 \lambda_{0,i}^2}\left[\frac{(\tilde{\nu}_i - 1)}{\tilde{\nu}_i}\tilde{\boldsymbol{p}}_i'\right]' + \bar{\boldsymbol{f}}_i - \ddot{\tilde{\boldsymbol{p}}}_i - \bar{c}_i\,\dot{\tilde{\boldsymbol{p}}}_i \quad (i = 1, \dots, n), \qquad (12)$$

where $\tilde{\nu}_i$ corresponds to $\bar{\nu}_i$ in terms of the approximate solution. The unbalanced residuals can be minimized by ensuring that they are orthogonal in the nondimensional domain [0,1] to the trial functions adopted in the discretization. Finally, the approximate form of the vector-valued balance equations of the end effector can be obtained by substituting Eqns. (10) and (11) into Eqns. (8) and (9). The resulting set of ODEs is solved taking a direct approach, i.e., the force applied to the cables is considered the input while the EE trajectory/orientation and the cable shapes are the outputs. In this sense, the values of $\Lambda_i(t)$ are assigned by means of $\Lambda_i(\tau) = 1 - \left|\left|\hat{\boldsymbol{n}}_i\right|\right|$. To perform the time-integration of the ODEs, the system of algebraic equations resulting from the evaluation

Materials Research Proceedings **26** (2023) 387-392 https://doi.org/10.21741/9781644902431-63

of the governing equations of motion at $\tau = 0$ and considering zero initial acceleration and velocity is solved to obtain the initial values $\boldsymbol{q}_{i,j}(0)$. The initial values of $\Lambda_i(0)$ are computed so that the fulfill the equilibrium of the EE.

Simulation results and influence of the cable mass

To assess the impact of the cable mass in the behavior of a CDPR under real operational conditions, the following procedure is employed. First, a position control approach in the Cartesian space is designed using a very simple dynamic model for the robot, that assumes massless, inelastic cables, for simulating its behavior. Then, employing the same controller, the behavior of the robot is simulated using the dynamic model exposed and solved by the procedure described in the previous Sections. The control architecture is shown in Fig. 1, where $(\boldsymbol{p}_M, \theta_x)^*$ and $(\boldsymbol{p}_M, \theta_x)$ stand for the desired and the simulated EE trajectory, respectively. The redundancy of the actuation, i.e., the conversion between the desired EE acceleration $(\ddot{\boldsymbol{p}}_M, \ddot{\theta}_x)$ generated by the controller to the corresponding cable forces applied to the robot (T), is solved by means of the well-known Improved Closed Form proposed by Pott [7].

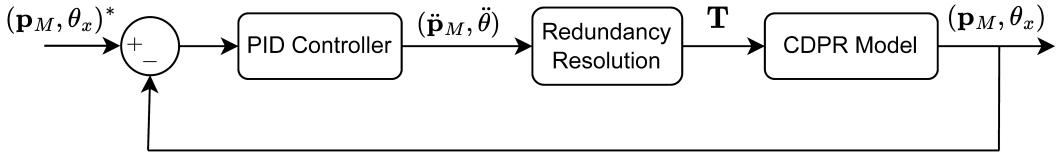

Figure 1. Block diagram of the control architecture

The PID gains are set by trial-and-error so that the position error committed with the massless cable model is less than 10mm. The set of ODEs is solved in Simulink using the classical Runge-Kutta (ODE4) method, with a sampling time of 1ms. The cable characteristics are $EA = 150360\,(\mathrm{N})$ and $\rho A = 4.19 \cdot 10^{-2}\,(\mathrm{kg/m})$ that correspond to those employed in [8]. An over-constrained CDPR with 4 cables and 3 DOF is considered. For the first case of study the robot frame is a rectangle of sizes $40 \times 10\,(\mathrm{m})$ and the EE geometry corresponds to a square of $0.5 \times 0.5\,(\mathrm{m})$. In case of study 2, the robot frame and EE are scaled by $1/4$. The EE mass is $M = 20\,\mathrm{kg}$ and its inertia $J = 0.833\,(\mathrm{kg{\cdot}m^2})$. The cable tension limits used for solving the redundancy by the Improved Closed Form are $[500,4000]\,(\mathrm{N})$. The employed trajectory is a circumference and the time evolution of $\boldsymbol{p}_M^*$ is generated by the interpolation algorithm detailed in [9]. For case of study 1 the radius is $r = 2.5\,(\mathrm{m})$ which is scaled proportionally for case of study 2. The maximum values for the EE linear speed, acceleration and jerk are, respectively $v = 12\,(\mathrm{m/s})$, $a = 27\,(\mathrm{m/s^2})$ and $j = 122\,(\mathrm{m/s^3})$, while for the second case these values are $v = 3\,(\mathrm{m/s})$, $a = 6.9\,(\mathrm{m/s^2})$ and $j = 30.6\,(\mathrm{m/s^3})$, which correspond to the same angular velocity of the EE describing the circumference in both cases. Fig. 2 shows the desired trajectory and the real one obtained for both cases of study. The legends MSC and MC stand for the results obtained with the massless and mass cable dynamic models, respectively. Analogously, Fig. 3 shows the tracking error and Fig. 4 shows the cable tension distributions generated.

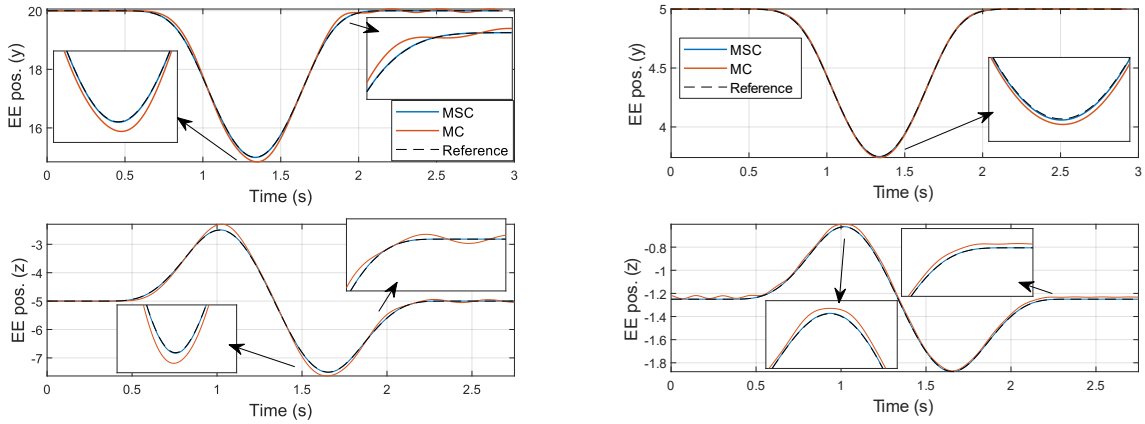

(a) Case 1 (b) Case 2

Figure 2. Position tracking

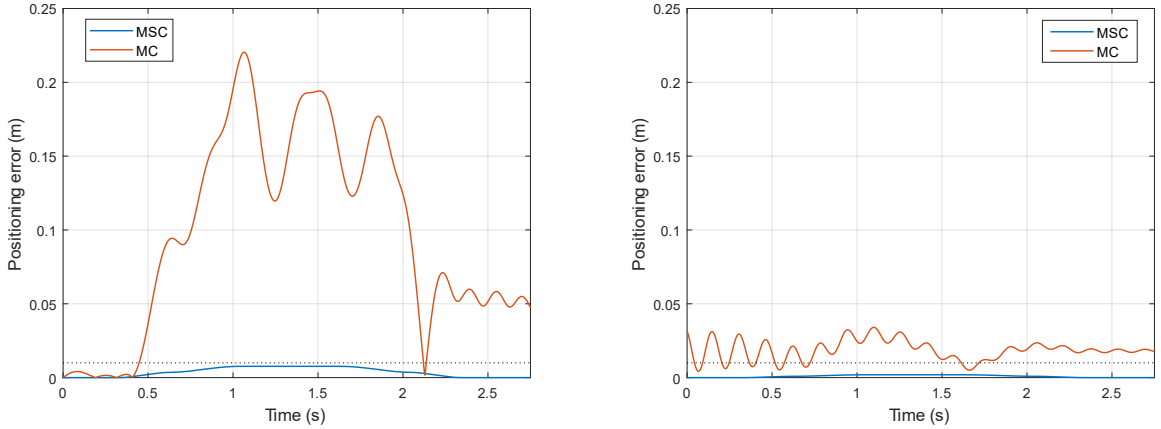

(a) Case 1 (b) Case 2

Figure 3. Tracking error

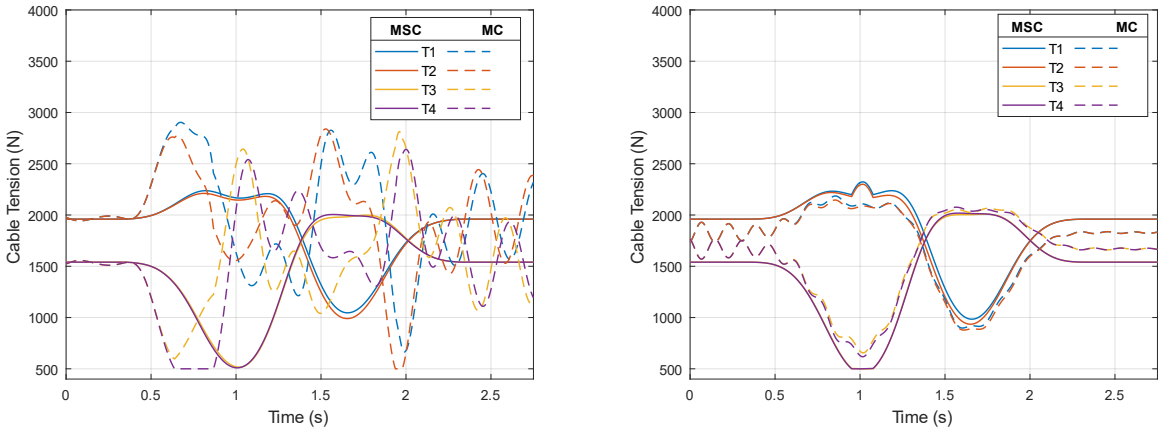

(a) Case 1 (b) Case 2

Figure 4. Cable tension distribution

In the case of study 1, it can be observed that using the controller designed considering a dynamic model with massless cables, yields to non-negligible differences between the expected and the real behavior of the robot, which is simulated by means of the proposed dynamic model when considering cable mass and elasticity. The tracking performance suffers a great deterioration as the maximum tracking error during the trajectory grows from less than 1 cm to more than 20

cm. Furthermore, the real cable force distribution presents an important change compared to the expected one, with considerable oscillations and values in the lower limit. On the other hand, we can see how that difference between the expected and the real behavior is considerably less in the case of study 2, as the robot size is 4 times smaller, therefore, cables total weight is reduced and therefore its effect on the robot dynamics, as expected.

Conclusions

In this work, a dynamic model for a planar CDPR with 3 DOF and n cables is proposed taking into account the effect of cables mass and elasticity. The system of partial differential equations corresponding to the cables motion is formulated, together with the boundary conditions imposed by the robot geometry and the ordinary differential equations that model the EE movement. A methodology based on the Garlekin discretization method is proposed to solve the system. Finally, the model is validated under a closed-loop position control strategy in the Cartesian space. The effect of the cables mass is assessed by comparing the results obtained under the same control strategy using the proposed model and a typical massless model. It can be concluded that the geometry of the robot is a key aspect to consider when deciding the level of complexity required for the CDPR model to be employed in model-based control strategies.

Acknowledgements

This research was in part sponsored by the NATO Science for Peace and Security Programme under grant id. G5924. Dr. Guillermo Rubio Gómez wishes to thank the University of Castilla-La Mancha for the financial support provided by the post-doctoral grant 2021-POST-20486.

References

[1] Pott, A.: Introduction. In: Cable-Driven Parallel Robots. Springer Tracts in Advanced Robotics, pp. 1-13. Springer, Cham (2018). https://doi.org/ 10.1007/978-3-319-76138-1 1

[2] Castillo-Garcia, F. J., Juárez-Pérez, S., González-Rodriguez, A., Rubio-Gómez, G., Rodríguez-Rosa, D., Ottaviano, E. (2021) Closed loop cable robot for large horizontal workspaces. Smart Structures and Systems, An International Journal, 27(2), 397-406.

[3] Santos, J.C., Chemori, A., Gouttefarde, M.: Model predictive control of large-dimension cable-driven parallel robots. In: International Conference on Cable-Driven Parallel Robots, pp. 221-232 (2019). Springer. https://doi.org/10.1007/978-3-030-20751-9_19

[4] Merlet, J.-P., Tissot, R.: A panorama of methods for dealing with sagging cables in cable-driven parallel robots. In: Advances in Robots Kinematics (2022). https://doi.org/10.1007/978-3-031-08140-8_14

[5] Ottaviano, E., Arena, A., & Gattulli, V. (2021). Geometrically exact three-dimensional modeling of cable-driven parallel manipulators for end-effector positioning. Mechanism and Machine Theory, 155, 104102. https://doi.org/10.1016/j.mechmachtheory.2020.104102

[6] Arena, A., Ottaviano, E., Gattulli, V. (2023). Dynamics of Cable-Driven Parallel Manipulators with Variable Length Vibrating Cables. Journal of Sound and Vibration. *Under review*

[7] Pott, A.: An improved force distribution algorithm for over-constrained cable-driven parallel robots. In: Computational Kinematics, pp. 139-146. Springer (2014). https://doi.org/10.1007/978-94-007-7214-4_16

[8] Du, J., Agrawal, S.K.: Dynamic modeling of cable-driven parallel manipulators with distributed mass flexible cables. Journal of Vibration and Acoustics 137(021020), 1-8 (2015). https://doi.org/10.1115/1.4029486

[9] Fang, Y., Hu, J., Liu, W., Shao, Q., Qi, J., Peng, Y.: Smooth and time-optimal s-curve trajectory planning for automated robots and machines. Mechanism and Machine Theory 137, 127-153 (2019). https://doi.org/10.1016/j.mechmachtheory.2019.03.019